ARTICLE

Downstream process design for Gag HIV-1 based virus-like particles

Elianet Lorenzo[1] | Laia Miranda[1,2] | Francesc Gòdia[1] | Laura Cervera[1]

[1]Departament d'Enginyeria Química Biològica i Ambiental, Universitat Autònoma de Barcelona, Bellaterra, Spain

[2]University College London, London, UK

Correspondence
Elianet Lorenzo, Departament d'Enginyeria Química Biològica i Ambiental, Universitat Autònoma de Barcelona, Bellaterra, Spain.
Email: elianet.lorenzo@uab.cat

Abstract

Virus-like particles-based vaccines have been gaining interest in recent years. The manufacturing of these particles includes their production by cell culture followed by their purification to meet the requirements of its final use. The presence of host cell extracellular vesicles represents a challenge for better virus-like particles purification, because both share similar characteristics which hinders their separation. The present study aims to compare some of the most used downstream processing technologies for capture and purification of virus-like particles. Four steps of the purification process were studied, including a clarification step by depth filtration and filtration, an intermediate step by tangential flow filtration or multimodal chromatography, a capture step by ion exchange, heparin affinity and hydrophobic interaction chromatography and finally, a polishing step by size exclusion chromatography. In each step, the yields were evaluated by percentage of recovery of the particles of interest, purity, and elimination of main contaminants. Finally, a complete purification train was implemented using the best results obtained in each step. A final concentration of 1.40×10^{10} virus-like particles (VLPs)/mL with a purity of 64% after the polishing step was achieved, with host cell DNA and protein levels complaining with regulatory standards, and an overall recovery of 38%. This work has resulted in the development of a purification process for HIV-1 Gag-eGFP virus-like particles suitable for scale-up.

KEYWORDS
chromatography, clarification, downstream processing, HIV-1 Gag-eGFP VLP, nanoparticle quantification

1 | INTRODUCTION

Vaccines stimulate the immune system allowing the individual itself to develop defense mechanisms against a specific agent. Among the different types, virus-like particles (VLPs)-based vaccines have been gaining interest in recent years as they can trigger both humoral and cellular immune responses (Fuenmayor et al., 2017; Nooraei et al., 2021).

The manufacturing of these particles includes their production by cell culture followed by their purification to meet the requirements of its final use (Mittal et al., 2022; Vicente et al., 2011). Downstream processing (DSP) of nanoparticles is still a challenge. Although filtration and centrifugation techniques are scalable to a certain extent and often used in industrial scale for vaccine and gene therapy products manufacturing, they are labor-intensive and requiring

WILEY

expensive equipment (in the case of centrifugation) (Moleirinho et al., 2019). Consequently, in the past few years, the focus has been moving to chromatography and membrane-based separation techniques (Kramberger et al., 2015).

Despite the efforts made in this field, it is known that even purified VLP preparations are contaminated with some extracellular vesicles (EVs) (González-Domínguez et al., 2021). They share very similar properties that make difficult to obtain final VLP formulations with high purity (Lavado-García et al., 2020).

Here, we propose the study of a purification process, specifically for enveloped HIV-1 Gag-eGFP VLPs (referred here as Gag VLPs). Based on the process reported by González-Domínguez et al. (2021), focussing on the evaluation of different operational units in each step of the DSP strategy, with the aim of improving the results previously obtained. This DSP proposal includes the study of the following steps: clarification, intermediate purification/concentration, capture chromatography, and polishing (Bandeira et al., 2012; González-Domínguez et al., 2021; Moleirinho et al., 2018). The best alternatives were determined considering the yield obtained in terms of recovery of Gag VLPs, the purity with respect to the total nanoparticles, including EVs, and the reduction of contaminating proteins and dsDNA. After selecting the best options in the different steps of the proposed DSP, a complete run was performed and characterized to demonstrate the output of the overall process.

As the target nanoparticles are produced extracellularly, the DSP process is considered to start from supernatant with a clarification step (Mittal et al., 2022). It is necessary to remove cell debris, large particles, and aggregates. Dead-end disposable depth-filters are used in this step and have shown a high yield of the product of interest with a high impurity removal capacity (Besnard et al., 2016; González-Domínguez et al., 2021). Long-term storage at −80°C ensuing clarification is frequently necessary for large-scale processes, thus, a secondary clarification is sometimes required in DSP strategies to remove the precipitates and/or aggregates resulted from thawed sample. Following clarification, an intermediate purification or concentration step is commonly included in the DSP train. Ultrafiltration by tangential flow filtration (TFF) and multimodal chromatography (MC) are widely used (Lima et al., 2019; Moleirinho et al., 2018; Pereira Aguilar et al., 2020). Even when there is a bind-elution step afterward, the concentration step is beneficial for reducing loading times in chromatographic columns while increasing the concentration of loaded material (Moleirinho et al., 2018). The advantages of including an MC as intermediate purification step is the elimination of impurities that could interact with the resins/membranes, favoring a good capture of the molecule of interest in the following bind-elution steps (Lima et al., 2019; Reiter et al., 2020; Zaveckas et al., 2018).

Different chromatographic modes can be applied for capture and purification of these particles. Ion exchange chromatography (IEC) is commonly used to capture and concentrate VLPs. Anion exchange resins like CIMmultus QA Monolith, Mustang Q, and Capto Q ImpRes have been the most used for the purification of these nanoparticles with good yields and purity (Moleirinho et al., 2018;

Pereira Aguilar et al., 2020; Steppert et al., 2016) Moreover, a combination of different binding mechanisms, for example, hydroxyl-functionalized polymethacrylate monoliths is a type of chromatography that has been used in the purification of HIV-1 Gag VLPs (Steppert et al., 2017). Affinity chromatography (AC) has recently gained higher importance in biotherapeutics manufacturing field due to unique selectivity capacity (Bandeira et al., 2012; Segura et al., 2013; Zhao et al., 2019). It has been shown that viruses and VLPs can be purified efficiently using heparin AC (Reiter et al., 2019; Zhao et al., 2019). However, after this capture step, usually, it is necessary to perform a polishing step. Size-exclusion chromatography (SEC) and ultrafiltration/diafiltration are the most used alternatives at this stage (Moleirinho et al., 2018; Nweke et al., 2017; Vicente et al., 2011).

2 | MATERIALS AND METHODS

All reagents were acquired from Sigma Aldrich, unless otherwise mentioned.

2.1 | Cell culture conditions

HEK293SF-3F6 cells, kindly provided by Dr. Amine Kamen from McGill University, were cultured in HyCell TransFx-HTM (Hyclone) medium supplemented with 2% GlutaMAXTM (Gibco, Thermo Fisher Scientific) and 0.1% PluronicTM (Gibco, Life Technologies, Thermo Fisher Scientific). Cells were routinely maintained in disposable polycarbonate Erlenmeyer flasks (Corning), and incubated at 37°C, 5% of CO_2, 85% relative humidity, and 130 rpm. Cell quantification and viability were determined with the automated cell counter NucleoCounter® NC-3000™ (Chemometec).

2.2 | Plasmid

Pr55Gag polyprotein sequence from the pCMV55M1-10 plasmid (Schwartz et al., 1992) was introduced into the pEGFP-N1 plasmid (Clontech). The resultant plasmid (pGag-eGFP), coding for a Rev-independent HIV-1 Gag protein fused in frame to the enhanced GFP, can be found in the NIH AIDS Reagent Program (Cat #11468).

2.3 | VLP production by transient transfection

HEK293SF-3F6 cells were transfected at $1.8–2 \times 10^6$ cells/mL, and viability greater than 90%. In essence, the DNA at a final concentration of 1 µg/mL was added into fresh culture medium and vortexed for 10 s. The transfection reagent PEIpro® (Polyplus-transfection SA) at a DNA:PEI ratio of 1:2 w/w was then added. The mix was vortexed three times for three seconds and incubated for 15 min at room temperature. Last, formed complexes were added

into the cell culture. Medium was also supplemented with 3.36 mM valproic acid and 5.04 mM caffeine 4 h posttransfection to increase cell productivity upon transient gene expression (Cervera et al., 2015). Culture was stopped at 72 hpt to maximize VLP yields. To measure the transfection efficiency, the percentage of GFP-positive cells was assessed using a BD FACS Canto II flow cytometer (BD Biosciences).

2.4 | Filtration equipment

Filtration experiments were performed using an automated Spectrum® KrosFlo® Research 2i TFF System (Repligen).

2.4.1 | Clarification

Cell culture was stopped at 72 hpt, and after 2 h of sedimentation, bulk clarification of the supernatant was directly performed from the shake flask (González-Domínguez et al., 2021). Each filter was preequilibrated with PBS (Hyclone) before filtration. For primary clarification, MilliStak®+ D0HC μpod®+ depth filter (Merck), and Supracap™ 50V100™ depth filter capsules (Pall Corporation) were compared. The liquid supernatant after cell sedimentation (1L) was loaded to each filter tested. MasterFlex® 96410-13 silicon tubes (Cole-Parmer) were connected to the filter inlet and outlet; and a pressure sensor (Cole-Parmer) connected to the filter inlet. The filtration flux was set to 5 mL·min^{-1} for the MilliStak®+ D0HC μpod®+ depth filter and 4 mL·min^{-1} for the Supracap™ 50V100 depth filter capsules. After selection of the primary clarification filter, 500 mL clarified bulk was used as secondary clarification feed. For secondary clarification, the used filters were Sartopore® SartoScale 25 PP3® (Sartorius AG) and Supor® EAV—Mini Kleenpak™ 20® filter capsules (Pall Corporation). Their filtration flux was set to 5 mL·min^{-1} and the same experimental setup was used. After filtration, the syringe filters were emptied with air to recover all the product. Culture supernatant was either stored at 4°C or frozen at −80°C for long-time storage. The turbidity of the clarification samples was measured using a portable turbidimeter (Thermo Fisher Scientific).

2.4.2 | TFF

The ultrafiltration step was performed using a Centramate Cassette with a 300 kDa molecular weight cut-off (MWCO) membrane (Pall Corporation). The omega PES membrane had an effective filtration area of 0.02 m^2. Before starting, the membrane was sanitized with 1 M sodium hydroxide (NaOH), neutralized with ultrapure water, and preconditioned with PBS 1X. A factor of concentration of 10 times starting with 2L of sample (clarified cell culture supernatant) and a flux of 35 mL·min^{-1} were selected. Transmembrane pressure was maintained at 0.6 bar approximately. After filtration, the membrane was sanitized with 0.5 M NaOH overnight and neutralized with ultrapure water.

2.5 | Preparative chromatography

2.5.1 | Chromatographic system

Chromatographic runs were performed using an Äkta Pure 25M2 system (Cytiva, GE Healthcare Live Sciences) with a S9 sample pump and a F9-C fraction collector, equipped with a 1.4 mL mixer chamber. System control, data acquisition, and analyses were performed using the Unicorn 6.4.1 software (Cytiva, GE Healthcare Live Sciences). UV absorbance (280, 260, and 488 nm wavelengths), pressure, pH, and conductivity were continuously monitored.

2.5.2 | Chromatography media and mobile phases

All preparative chromatographic experiments for Multimodal and Ion Exchange were performed using 50 mM HEPES, pH 7,2 as mobile phase A and 50 mM HEPES, 2 M NaCl, pH 7,2 as mobile phase B. In case of Hydrophobic interaction, it was also used 50 mM HEPES, pH 7.2 as mobile phase A, but 50 mM HEPES, 1.5 M (NH$_4$)$_2$SO$_4$, pH 7.2 as mobile phase B. The Capto heparin was performed with 0.1 M Tris, 0.01 M Citric Acid, 0.23 M NaCl, pH 7.4 as mobile phase A and 0.1 M Tris, 0.01 M Citric Acid, 2M NaCl, pH 7.4 as B. For POROS heparin was used at 50 mM in Tris-HCL, pH 7.5 as mobile phase A and 50 mM Tris-HCL, 2 M NaCl, pH 7.5 as mobile phase B. Different concentrations of the modifier (NaCL or (NH$_4$)$_2$SO$_4$) were obtained by mixing mobile phases A and B using the chromatography system. For SEC experiments a formulation solution (FS) composed of 20 mM NaH$_2$PO$_4$, 50 mM NaCl, 2 mM MgCl$_2$, 2% Sucrose, pH 7.5 was used as mobile phase. If not further stated, cleaning in place was performed using 1 M NaOH solution in MC, IEC and HIC, 0.1 M NaOH in AC and 0.5 M in SEC. The chromatography media tested are summarized in Table 1. All materials were used for a single cycle.

2.5.3 | Intermediate purification, capture, and polishing of GagVLPs

For the intermediate purification and capture of Gag VLPs, clarified HEK293 cell culture supernatant from different produced batches was directly loaded onto the prepacked columns/membranes HiScreen Capto Core 700, CIMmultus Monolith QA, Mustang QXT Acrodisc, HiScreen Capto Q ImpRes, HiTrap Capto Heparin, and manually packed XK16/20 POROS Heparin. The sample loaded into CIMmultus Monolith OH$^-$ was previously diluted 1:2 with 50 mM HEPES, 3 M (NH$_4$)$_2$SO$_4$, pH 7,2. Polishing after capture step was performed with two desalting columns. A prepacked HiTrap Sephadex G-25 and a manual packed XK 16/40 Sepharose 4 fast flow (4FF). In the cases of manual packed columns, the packing protocol was performed following the instructions suggested by the manufacturer. In all cases, the flow rates used were those recommended by the manufacturers. In all chromatographic experiments, equilibration of the stationary phase was performed before

TABLE 1 Chromatography media is used for preparative chromatography.

Type of chromatography		Type of column and name	Manufacturer	Column volume (mL)
Multimodal	Agarose-based core beads	HiScreen Capto Core 700	Cytiva	4.7
Ion exchange	Polymethacrylate-based monolithic column	CIMmultus Monolith QA	Sartorius AG	1
	Polypropylene-based membrane	Mustang QXT Acrodisc	Pall Corporation	0.86
	High-flow agarose-based beads	HiScreen Capto Q ImpRes	Cytiva	4.7
Hydrophobic interaction	Polymethacrylate-based monolithic column	CIMmultus Monolith OH⁻	Sartorius AG	1
Affinity (heparin)	Agarose-based beads	HiTrap Capto Heparin	Cytiva	1
	Cross-linked poly(styrene-divinylbenzene)	XK 16/20 POROS Heparin	Thermo Fisher Scientific	5.6
Size exclusion	Cross-linked dextran-based beads	HiTrap Sephadex G-25	Cytiva	5
	Highly cross-linked 4% agarose-based beads	XK 16/40 Sepharose 4 Fast Flow	Cytiva	48

loading using the corresponding equilibration buffer. After loading, columns were washed with equilibration buffer to ensure the removal of unbound material from the column. In MC, elution was achieved by a 100% buffer B. In capture experiments, elution was achieved by salt step gradients. In SEC step, Gag VLPs were eluted with the FS in the void volume. Details of flow rates, loading volumes, and elution gradients are summarized in Table 2. After the elution phase, columns were regenerated using 100% B buffer. Fractions were collected and pooled according to the chromatograms, considering the UV absorbance signals of 280, 260, and 488 nm.

2.6 | Western blot and SDS-PAGE

Forty microliters of sample were mixed with 20 μL of 4x LDS Sample Buffer and 7 μL of 2M DTT, followed by 20 min incubation at 96°C. Stored at 4°C until gelled, 20 μL of each sample were loaded onto precast NuPAGE Bis/Tris gels 4%–12% (Invitrogen). Five microliters of SeeBlue® Plus2 Prestained Protein Standard (Invitrogen) was used as low molecular weight control. Gels were run at 200 V, 400 mA, 45 min, in MES-SDS running buffer. For SDS-PAGE gels, proteins were stained with Coomassie Brilliant Blue G-250 based EZBlueTM Gel Staining Reagent (Sigma Aldrich). For Western blot analysis, proteins were transferred onto 0.2 μm nitrocellulose membranes using the Trans-Blot® turbo system (Bio-Rad Laboratories). Membranes were blocked with PBS 5% (w/v) nonfat dry milk for 30 min, washed with PBS 0.1% (w/v) Tween-20, and then incubated overnight at 4°C with the primary monoclonal antibody against HIV-1 p24 (dilution 1:2000 in PBS) (Icosagen AS). After washing, product immunodetection was performed with an antimouse IgG antibody conjugated with an alkaline phosphatase (dilution 1:5000 in PBS 1X), incubated 2 h at room temperature, and washed with PBS 0.1% (w/v) Tween-20. For protein bands visualization, the

membranes were incubated with NBT-BCIP solution for 2–3 min. The enzymatic reaction was stopped with ultrapure water.

2.7 | Nanoparticle tracking analysis (NTA)

NTA was used to determine particle size distribution and particle concentration. NanoSight® NS300 device (Malvern Panalytical) equipped with a blue laser module (488 nm) to quantify HIV-1 Gag-eGFP VLPs, and a neutral density filter for total particle quantification by light scattering. Samples were serially diluted in particle-free water to achieve a concentration of 20–80 particles per video frame (the instrument's linear range). For the injected samples, three replicates of each dilution were measured at 22°C, with a viscosity of 0.9 cP, and three videos of 60 s length were acquired. Capture settings were recorded with an sCMOS camera, setting the screen gain to 1, manually adjusting the camera level before each measurement (eight for samples containing Gag-eGFP VLPs and 11 for controls), and setting a detection threshold of 4. The remaining analysis parameters were automatically selected by the software and kept constants for all samples. Data were acquired and processed with the NanoSight NTA software version 3.2.

2.8 | Fluorescence intensity measurements

The fluorescence intensity was measured in a Cary Eclipse Fluorescence Spectrophotometer (Agilent Technologies) to determine the concentration of Gag-eGFP VLPs. The settings were λexcitation = 488 nm (slit = 5 nm) and λemission = 510 nm (slit = 10 nm). The relative fluorescence unit (RFU) values were calculated by subtracting the obtained fluorescence intensity (FU) values from the non-transfected negative control samples. An in-house developed and

TABLE 2 Parameters used in the chromatography experiments.

Type of chromatography	Flow rate (mL/min)	Column volume (mL)	Residence time (min)	Loaded material[a]	Loaded volume (mL)	Equilibration and wash	Step gradient elution
MC Capto Core 700 (Lagoutte et al., 2016; Reiter et al., 2020)	1.2	4.7	3.92	8.53E+11	70,5	6% B in 5CV	100% B in 10CV
IEC Monolith QA (Pereira Aguilar et al., 2020; Steppert et al., 2016)	1	1	1.00	4.44E+12	120	5% B in 5CV	15%, 35%, 45%, and 65% B in 20CV
IEC Mustang Q (Carvalho, Silva, et al., 2019; González-Domínguez et al., 2021)	0.8	0.86	1.08	3.6E+12	240	5% B in 5CV	15%, 35%, 45%, and 65% B in 20CV
IEC Capto Q ImpRes (Moleirinho et al., 2019)	1.2	4.7	3.92	7.0E+11	70,5	6% B in 5CV	15%, 35%, 45%, and 65% B in 20CV
HIC Monolith OH⁻ (Steppert et al., 2017)	1	1	1.00	5.7E+11	77	100% B in 5CV	100%, 65%, 0% B in 20CV
AC Capto Heparin (Pereira Aguilar et al., 2020; Reiter et al., 2019)	1	1	1.00	8.1E+11	45	5% B in 8CV	12%, 25%, 50% B in 10CV
AC POROS Heparin (Zhao et al., 2019)	2	5.6	2.80	1.4E+12	100	5% B in 5CV	15%, 35%, 45%, and 65% B in 20CV
SEC Sephadex G- (Cervera et al., 2017)	1	5	5.00	9.20E+10	0,5	FS in 5CV	100% FS in 2CV
SEC Sepharose 4 FF (Carvalho, Silva, et al., 2019; González-Domínguez et al., 2021)	1	48	48.00	1.78E+12	5	FS in 5CV	100% FS in 2CV

Abbreviations: AC, affinity chromatography; B, buffer corresponding to mobile phase B; CV, column volume; FS, formulation buffer; HIC, hydrophobic interaction chromatography; IEC, ion exchange chromatography; MC, multimodal chromatography; SEC, size exclusion chromatography.

[a]Load material is referred to total nanoparticles (including Gag VLPs and EVs) quantify by NTA.

validated quantification assay was used to convert RFU values to Gag-eGFP concentration values (Cervera et al., 2013).

2.9 | Total protein and dsDNA quantification

Host cell protein concentration was determined using the Micro BCA protein assay kit, according to the manufacturer's instructions. Briefly, serial PBS-buffer dilutions (between 2- and 256-fold) of standard and samples were dispensed into the wells. After adding 150 μL of the Micro BCA working reagent into each well, plates were incubated for 1 h at 37°C. The bovine serum standard curve ranged from 1.5 to 200 μg/mL, and the absorbance was measured at 562 nm in the Victor 3 reader (Perkin Elmer). Protein concentration of the samples was determined using the standard curve.

Host cell DNA concentration was determined using the Quant-itTM Picogreen dsDNA assay kit, according to the manufacturer's instructions. Briefly, serial TE 1X- buffer dilutions (between 2 and 256-fold) of standard and the samples were dispensed into 96-well microplates. After adding 100 μL of the Quant-iTTM PicoGreen® reagent (dilution 1:1000) into each well, plates were incubated for 5 min at room temperature. The dsDNA standard curve ranged from 1.5 to 500 μg/mL, and the absorbance was measured on the Victor 3 (Perkin Elmer), prior and later to the Quant-iTTM PicoGreen® reagent addition since HIV-1 Gag-eGFP VLPs emit at the same range. The settings were λexcitation = 480 nm and λemission = 520 nm. DNA concentration of the samples was determined using the standard curve and subtracting the native fluorescence.

2.10 | Flow virometry analysis

Concentration of Gag-eGFP fluorescent events was quantified using a CytoFLEX LX (Beckman Coulter), equipped with a 405 nm filter. The threshold of the trigger signal (VSSC) was manually adjusted to 1500, and gains were set as 9, 95, and 115 for VSSC, FSC, and B525-FITC lasers, respectively. Samples were diluted with PBS 1X until an abort rate value below 2% was achieved. A total of 300,000 events were analyzed at a flow rate of 10 μL/min per sample. VSSC-H versus B525-FITC density plots were used to gate the different particle populations. Gating was adjusted manually for each channel. Events after 50 s were taken for analysis. The results were analyzed with CytExpert software.

2.11 | Dynamic light scattering

The dynamic light scattering technique was used to determine the size of HIV-1 Gag-GFP VLPs. The measurements were carried out at 25°C in a Zetasizer Nano ZS instrument (Malvern Instruments), equipped with a He/Ne 633 nm laser at 173°C. One hundred microliters of the sample were placed in disposable plastic cuvettes. Three consecutive measurements of each sample with 10–15 scans

of 10 s were performed for each independent measurement. The hydrodynamic diameter (MHD), particle size distribution in volume, derived count rate, and polydispersity index (PDI) average results were automatically obtained.

3 | RESULTS AND DISCUSSION

3.1 | Gag VLPs production and clarification step

To produce enough particles to evaluate the different alternatives in the DSP strategy, different HEK 293 cell culture batches were transfected. At 72 hpt (Cervera et al., 2017), there was a transfection efficiency in each batch around ~80%

After removal of cells by sedimentation, the first step in the DSP strategy is critical to improve the subsequent purification steps and consists in the clarification. For this step, two depth-filters were evaluated regarding Gag VLPs recovery and enrichment in respect to the total number of nanoparticles, and the reduction of main proteins and dsDNA contaminants. These parameters were referred to the loaded sample in each case. Supporting Information: Table S2 shows the results regarding two the parameters evaluated.

The DLS profile followed the same trend in both cases, although the peak was slightly higher for the Supracap™ 50V100 depth filter since there was a lower loss of Gag VLPs (Figure 1a). The smaller peak of the supernatant seen on the right may be due to cell debris or aggregates, which was diminished by the clarification. Electrophoresis confirmed the presence of a band greater than 75 kDa (the molecular weight of Gag-eGFP is approximately 88 kDa), confirmed to be Gag-eGFP, either free monomer or forming part of VLPs, by Western blot (Figure 1b).

Higher recovery and purity were achieved with the Supracap™ 50V100 depth filter. One possible explanation is the difference in nominal retention rating. The Supracap™ 50V100 depth filter has a nominal filter retention range between 2 and 4 μm; and the MilliStak®+ D0HC μpod depth filter has a nominal filter retention between 0.5 and 10 μm approximately (Carvalho, Silva, Moreira, et al., 2019). This implies that more heterogenous particles in size can pass through the MilliStak®+ D0HC μpod depth filter and they can also retain VLPs. It can be observed in the DLS data that the sample from MilliStak®+ D0HC μpod depth filter has a wider size distribution than the sample from Supracap. Higher recoveries of Gag VLPs were achieved in previous studies using the MilliStak®+ D0HC μpod depth filter (Boix-Besora et al., 2022; González-Domínguez et al., 2021). A possible cause could be that in both reported cases a lower amount of Gag VLPs was loaded compared to the amount loaded here, however, it has been previously demonstrated that clarification based on nominal filtration processes performs fairly well with recovery yields of around 80%, which is consistent with our results (Carvalho, Silva, Moleirinho, et al., 2019).

It should also be considered that a secondary clarification in DSP strategies is sometimes required. An additional clarification step is added in case that a previously frozen sample was to be used and

precipitates and/or aggregates appear during its thawing. The turbidity of the sample is an indication of how necessary it is to clarify again before continuing with the subsequent chromatography steps. For that reason, two different filters were evaluated (Sartopore® SartoScale 25 PP3 and Supor® EAV—Mini Kleenpak™ 20 filters) in case this step needs to be included in the purification process. The same parameters analyzed in the case of primary clarification were also considered in these experiments and the results were summarized in Supporting Information: Table S3. Figure 2a shows the DLS results of both clarified materials, where a similar profile is observed. The presence of Gag-eGFP was confirmed by SDS-PAGE and Western blot at the expected molecular size (Figure 2b).

The null enrichment of Gag VLPs in the secondary clarification could be because conventional filtration does not serve to enrich the preparation with Gag VLPs in respect to the total nanoparticles, since the large particles have already been removed by depth filtration. Moreover, although both filters reduced the amount of dsDNA respect to the load, it appears that the Supor® EAV—Mini Kleenpak™ 20 filter had some selectivity for dsDNA and certain proteins since the observed reduction was higher compared to Sartopore® SartoScale 25 PP3 filter. Although the GagVLPs did not increase with respect to total particles, it was possible to remove part of the contaminants, obtaining an optimal sample characteristics that allows a better performance of the column for the next chromatographic step (Besnard et al., 2016).

The best results in primary clarification were obtained with the Supracap™ 50V100 depth filter. Regarding secondary clarification, the Supor® EAV—Mini Kleenpak™ 20 filter was selected as the best option, if required. The selected method offers a robust approach for
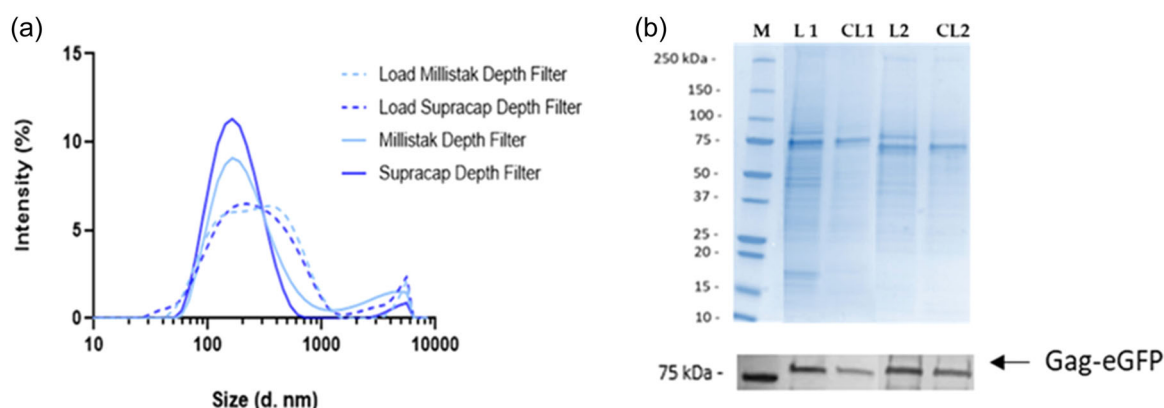
FIGURE 1 Primary clarification of Gag virus-like particles (VLPs) supernatant. (a) Dynamic light scattering (DLS) analysis of the MilliStak®+ D0HC μpod depth filter load (polydispersity index [PDI] = 0.439, hydrodynamic diameter [MHD] = 223.8), MilliStak®+ D0HC μpod depth filter clarified PDI = 0.387, MHD = 195.6), Supracap™ 50V100 depth filter load (PDI = 0.457, MHD = 242.3), Supracap™ 50V100 depth filter clarified (PDI = 0.239, MHD = 161.2). (b) SDS-PAGE and p24 Western blot of the depth filtration runs. M, molecular weight standard; L1 and L2, Load samples using for test MilliStak®+ D0HC μpod depth filter and Supracap™ 50V100 depth filter respectively; CL1 and CL2, clarified samples corresponding to MilliStak®+ D0HC μpod depth filter and Supracap™ 50V100 depth filter, respectively.
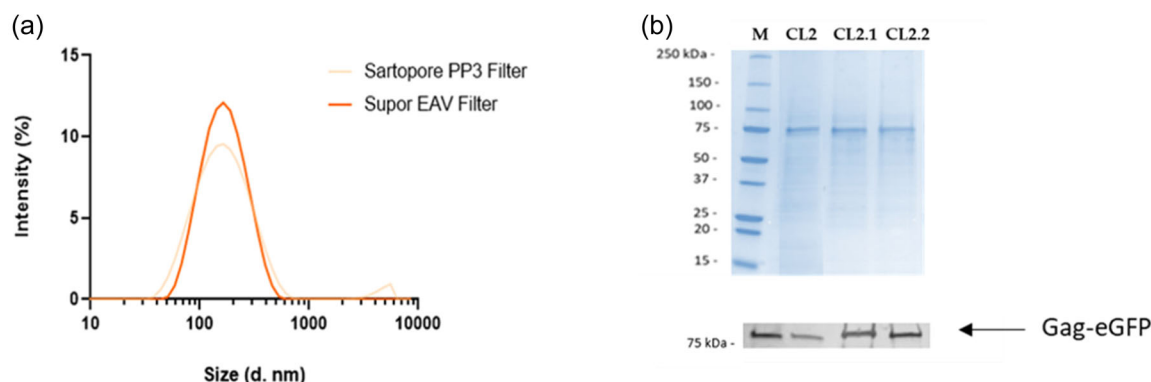
FIGURE 2 Secondary clarification of Gag virus-like particles (VLPs). (a) Dynamic light scattering (DLS) analysis of the Sartopore® SartoScale 25 PP3 filter clarified (PDI = 0.329, MHD = 137.8), Supor® EAV—Mini Kleenpak™ 20 filter clarified (PDI = 0.321, MHD = 143.3). (b) SDS-PAGE and p24 Western blot of the filtration runs, using a Sartopore® SartoScale 25 PP3 and a Supor® EAV—Mini Kleenpak™ 20 filters. PDI, polydispersity index; MHD, mean hydrodynamic diameter; M, molecular weight standard, CL2, Load sample using for test both filters; CL2.1 and CL2.2, clarified samples corresponding to Sartopore® SartoScale 25 PP3 filter and a Supor® EAV—Mini Kleenpak™ 20 filters, respectively.

the clarification of GagVLPs. Similar results were reported (Carvalho, Silva, Moreira, et al., 2019) for the clarification of influenza VLPs produced in insect cells.

3.2 | Intermediate step

Following clarification, a concentration step is often included in a purification process. It is very useful when the volume of the starting material is high, and it is also a step that allows the removal of contaminants (Moleirinho et al., 2018; Vicente et al., 2011). For that reason, in this work we evaluated a TFF 300 kDa PES membrane. In this case, the operation was characterized considering all the parameters evaluated in the previous steps (Supporting Information: Table S4).

All Gag VLPs have been recovered and concentrated 10-fold, with presence of some aggregates and a shift in the particle size as shown by the DLS profile (Figure 3a). However, when this sample was diluted and analyzed by NTA, although the presence of aggregates was also observed, the particle size obtained for the Gag VLPs was 146 nm, which corresponds to the expected results for these nanoparticles. In the electrophoresis (Figure 4f), a band greater than 75 kDa could be seen in the retentate, which did not appear in the permeate (data not shown). It was confirmed that this band corresponds to Gag-eGFP by Western blot (Figure 3b).

T-Series cassettes with omega polyethersulfone (PES) membrane, and molecular weight cut-off of 1000 and 300 kDa, have been reported for VLPs concentration enabling a removal of >80% of proteins while recovering approximately 60%–80% of VLPs (Lin et al., 2015; Venereo-Sanchez et al., 2016). In this case, ultrafiltration/diafiltration using TFF mode to concentrate Gag-eGFP VLPs is proposed as an intermediate step in DSP train with better results than previously reported (Nooraei et al., 2021; Venereo-Sanchez et al., 2016).

Another alternative to follow in this intermediate purification step is the use of a MC. In this work the HiScreen Capto Core 700 column was evaluated considering the parameters described (Supporting Information: Table S5). The mass balance results suggest that most of the contaminating proteins in the evaluated sample have a high molecular weight, and therefore, 88% remain in the FT together with the Gag VLPs (Reiter et al., 2019). A narrower profile was observed by DLS (Figure 3a), with a lower PDI and MHD, which indicated the presence of less aggregates in the FT fraction, which was then later confirmed to be Gag-eGFP by Western blot (Figure 3b).

In previous reports, a yield of 90.9% has been reported in the purification of Zika VLPs (Lima et al., 2019), 89.7% for yellow fever VLPs (Lima et al., 2019) and 89% for influenza VLPs (Lagoutte et al., 2016). However, it must be considered that for HIV-1 Gag VLPs a maximum of 73.1% recovery has been reported (Reiter et al., 2019), close to the results obtained here. In respect to other studies, although similar residence times and loading volumes were evaluated, the total number of nanoparticles loaded to the column was lower (Lagoutte et al., 2016; Lima et al., 2019; Reiter et al., 2019). Possibly this could be the cause of the low recovery percentages and reduction of contaminating proteins observed.

3.3 | Capture step

The evaluation of the capture step included six different chromatography methodologies: three based on ion exchange, one based on hydrophobic interactions and two based on heparin affinity. The characteristics of the samples loaded in the six chromatographies are summarized in Supporting Information: Table S1. All runs were analyzed considering the parameters described above for the other steps.
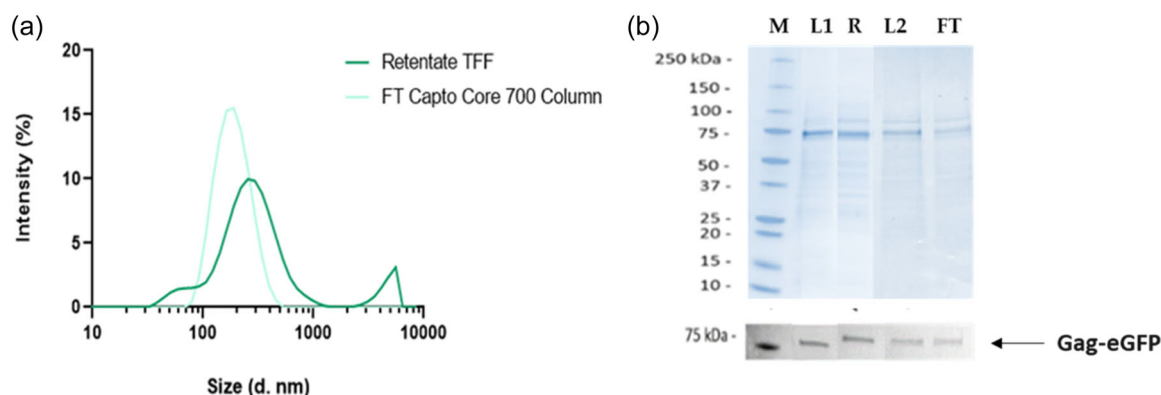
FIGURE 3 Tangential flow filtration (TFF) and multimodal chromatography experiments for concentration and intermediate purification of Gag virus-like particles (VLPs). (a) Dynamic light scattering (DLS) analysis of the TFF retentate PDI = 0.501, MHD = 241.8), FT Capto Core 700 column PDI = 0.166, MHD = 165.2); (b) SDS-PAGE and p24 Western blot of the filtration run with a 300 kDa PES membrane by TFF, and a chromatographic run with a Capto Core 700 column. PDI, polydispersity index; MHD, mean hydrodynamic diameter; M, molecular weight standard; L load sample used in TFF and MC; R, retentate sample resulted from TFF; FT flow through obtain in MC.

Among several chromatographic techniques, IEC has been already used to purify VLPs. Here, three IEC columns were tested: Monolith QA, Mustang Q, and Capto Q ImpRes. In all the cases, the fractions obtained during the runs were analyzed from the corresponding chromatogram. The second step in the elution phase fraction (named E2) was considered the main product fraction due to the higher GagVLPs concentration and simultaneous lower total protein and dsDNA content (Supporting Information: Figure S2). The E2 fraction, corresponds to conductivity values of 45–55 mS/cm. Similar elution conditions for VLPs have been reported (Pereira Aguilar et al., 2019; Steppert et al., 2016). Therefore, the subsequent comparative analyses were performed focusing on the E2 fraction.

In the Monolith QA chromatographic run the results achieved are summarized in Supporting Information: Table S6. According to our findings this method can separate the main impurities including host cell protein and DNA. The recovery of Gag VLPs, in the main elution fraction is less than 50%, however these results are comparable to data previously reported (Pereira Aguilar et al., 2020; Steppert et al., 2016).

For the Mustang Q, the mass balance results are show in Supporting Information: Table S7. Here, an improvement in yield with the Mustang Q compared to previously reported results was obtained (Boix-Besora et al., 2022; González-Domínguez et al., 2021). A possible explanation for this could be that, in this case, the loaded sample had been previously clarified using both filters, Supracap™ 50V100 and Supor® EAV—Mini Kleenpak, which allows a better performance of the membrane reducing as many precipitates as possible in the sample and avoiding system overpressure. In addition,
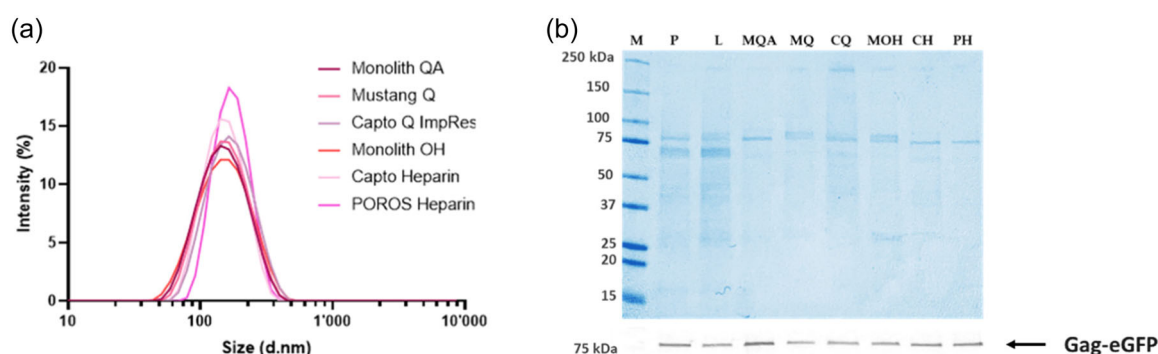
FIGURE 4 Purification of Gag virus-like particles (VLPs) by an ion exchange, hydrophobic interaction, and affinity chromatography. (a) Dynamic light scattering (DLS) analysis of the E2 fraction of the Monolith QA column (PDI = 0.190, MHD = 137.9), Mustang Q column (PDI = 0.176, MHD = 135.5) and Capto Q ImpRes column (PDI = 0.151, MHD = 152.0), E3 fraction of the Monolith OH column (PDI = 0,18, MHD = 132), W fraction of the Capto Heparin column (PDI = 0,13, MHD = 140) and E1 of the POROS Heparin column (PDI = 0,1, MHD = 162,8). (b) SDS-PAGE and p24 Western blot of the production, load material and the GagVLPs main fraction of each chromatographic run. E1, E2, and E3 elution peaks from respective step gradient W, fraction corresponding to wash step; PDI, polydispersity index; MHD, mean hydrodynamic diameter; M, molecular weight standard, P, Supernatant production sample; L, load sample MQA, MQ, CQ, MOH, CH, PH, main fraction corresponding to Monolith QA, Mustang Q, Capto Q ImpRes Monolith OH, Capto Heparin and POROS heparin columns, respectively.
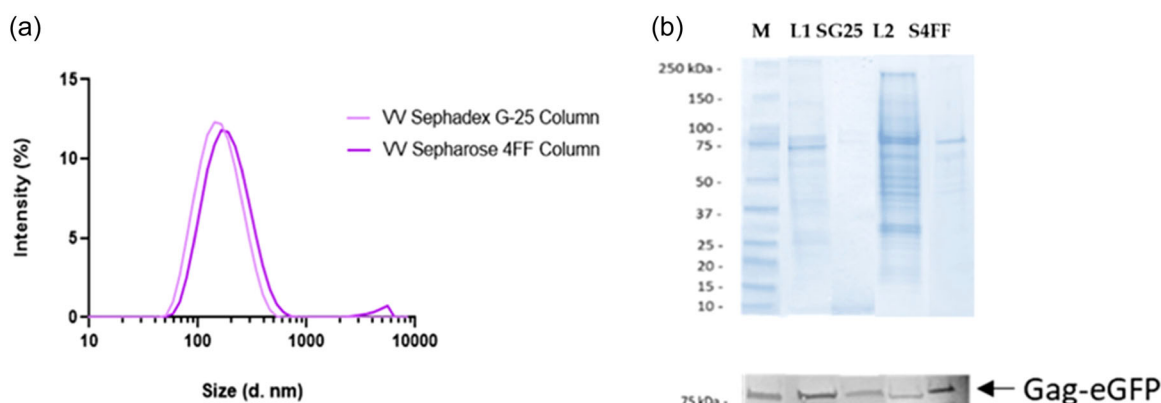
FIGURE 5 Purification of Gag virus-like particles (VLPs) by size exclusion chromatography. (a) Dynamic light scattering (DLS) analysis of the VV fraction of the Sephadex G-25 column (PDI = 0.174, MHD = 139.9), and Sepharose 4FF column (PDI = 0.217, MHD = 172.8). (b) SDS-PAGE and p24 Western blot of the chromatographic runs using a Sephadex G-25 column and a Sepharose 4FF column. MHD, mean hydrodynamic diameter; PDI, polydispersity index; VV, void volume; M, molecular weight standard; SG25, VV from Sephadex G-25 column; S4FF, VV from Sepharose 4FF column, L, loaded sample in SG25 and S4FF.

TABLE 3 Mass balance of Gag virus-like particles (VLPs) obtained from final downstream processing (DSP) validation run.

Sample	Volume (mL)	Total gag-eGFP VLPs	VLPs's recovery[a] (%)	Gag-eGFP VLPs/total particle (%)	Total protein (µg/mL)	Total protein reduction[a] (%)	dsDNA (ng/mL)	dsDNA reduction[a] (%)	Gag-eGFP protein (µg/mL)	Gag-eGFP/total protein (%)
Production	100	8.8×10^{11}	100	38	560.9	-	613	-	15.1	3
Clarified	100	7.9×10^{11}	90	43	550	2	217	65	10.2	2
E2 fraction CaptoQ ImpRes	2	6.04×10^{11}	76	60	542	98	488.4	96	175	32
VV fraction S4FF	6	8.4×10^{10}	55[b]	64	30.0	83	5.8	96	21	70
Overall[c]			38			100		100		

Note: Total particle, total protein, and dsDNA concentrations were measured by nanoparticle tracking analysis (NTA), BCA, and Picogreen assays, respectively. VV, void volume fraction; E2, step gradient elution peak 2; S4FF, Sepharose 4 fast flow.

[a]Refers to the recovered/reduced from the previous step.

[b]This percentage was calculated taking into account that the sample loaded in SEC was diluted four times.

[c]Final recovery/reduction of the entire process with respect to the initial sample (crude supernatant).

the concentration of loaded material in this case was lower than in the previously reports, which has also allowed better results.

Highest recovery was achieved using Capto Q ImpRes which allowed not only the separation of GagVLPs from host cell protein and dsDNA but also the enrichment respect to total nanoparticles (Supporting Information: Table S8). The yield obtained was similar when using the same resin for adenoviruses (~80%), according to previous reports (Moleirinho et al., 2018). These data support the use of strong quaternary amine ion exchangers to concentrate and purify HIV-1 VLPs.

The use of hydroxyl-functionalized polymethacrylate monolith as one more possibility in the capture step was also tested. The fraction corresponding to elution step 3 showed the highest content of Gag VLPs (22%). In this case the elution buffers used were different than in IEC experiments and the major Gag VLP concentration fraction presents conductivity values approximately of 20 mS/cm (Supporting Information: Figure S3c and Table S9). Similar results were reported regarding the recovery of Gag VLPs in two main elution peaks using this column (Steppert et al., 2017).

Regarding the enrichment of VLPs, no increase was observed, however, an almost total elimination of contaminating host cell proteins and DNA was observed (Supporting Information: Table S9). The overall advantages for macroporous polymethacrylate monoliths are well established (Jungbauer & Hahn, 2004). From the two types of functionalized monoliths tested, the best results were obtained with the Monolith QA, which suggests that the ion exchange principle provided by the QA ligand allows a better recovery of the Gag VLPs, compared to the hydrophobic exchanges provided by the OH ligand.

Several studies have shown the potential of heparin AC for the purification of VLPs allowing its separation from other nanoparticles populations (Reiter et al., 2019). Different chromatography media have been used to couple the heparin ligand (Zhao et al., 2019). Here, Capto heparin and POROS heparin columns were tested. In both cases it was observed a similar chromatographic profile where the fraction with higher amount of Gag VLPs elute at 20-25 mS/cm values of conductivity with high reduction of protein and dsDNA contaminants (Supporting Information: Figure S4). Despite these similarities, POROS heparin was superior in its ability to capture the Gag VLPs (Supporting Information: Tables S10 and S11). The results obtained show the effectiveness of this resin to separate the Gag VLPs from other nanoparticles present in the sample.

The PDI and MHD analyzed by DLS were very similar in all capture chromatography evaluated (Figure 4a). Also, it was observed in all the cases a band with the expected size by SDS-PAGE, confirmed to be Gag-eGFP by Western blot (Figure 4b).

Considering that the initial samples used for the tests were different, the main criteria of evaluation were based on the recovery of Gag VLPs, considering the total Gag VLPs/mL of column/ membrane loaded and eluted in each case. According to the obtained results, the Capto Q ImpRes column offers a better recovery of the product of interest, enriching its presence with respect to the rest of the nanoparticles, and at the same time maintaining low amounts of

contaminants. These parameters, together with the molecular characterization of the Gag-VLPs, make this column the optimal option for the capture and purification of the Gag VLPs.

3.4 | Polishing step

Polishing is a critical step to achieve a final clinical grade material. After capture step we evaluated size exclusion chromatography (SEC) as a polishing step with two different columns, HiTrap® Sephadex G-25 column, and a XK 16/40 Sepharose 4FF column. The same parameters as in the previous steps were used for characterization. In SEC, Gag VLPs elute in the void volume (VV) (Supporting Information: Figure S5). The mass balance results of both runs are summarized in Supporting Information: Tables S12 and S13. The PDI and MHD are very similar. Also, a band greater than 75 kDa was observed by electrophoresis and Western blot (Figure 5b).

The Sepharose 4 FF gave better results compared to the Sephadex G-25 column. A possible explanation could be the use of different resins, the difference in the column dimensions, or both (González-Domínguez et al., 2021). Even so, in this step, it was still possible to eliminate more dsDNA and total protein for both cases. This polishing step also has the advantage of enabling the exchange of the process buffer for a formulation or storage buffer (Peixoto et al., 2007) (Moleirinho et al., 2018).

3.5 | Evaluation of the optimized purification process

To finally validate the process, a 100 mL sample from a production batch was treated through the complete purification train, using the techniques showing a better performance at each step. First, clarification was performed using the Supracap™ 50V100 depth filter. Secondary clarification was not necessary, since the turbidity values were acceptable after the first filtration, which ruled out the presence of large aggregates and precipitates. The next step was capture with the HiScreen Capto Q ImpRes column. The TFF step was not included since in this case it was not necessary to concentrate the sample before chromatography. In general terms, it is suggested to consider the TFF step in the DSP train when it is necessary to concentrate the sample. After IEC, desalting was performed with XK 16/40 Sepharose 4FF column. The mass balance of this complete validation run is summarized in Table 3.

Furthermore, it can be noted that the VLPs obtained after the polishing step were in a formulation solution, which is an advantage for their subsequent lyophilization. The results obtained from the global yield of the process and the purity of the product of interest improved those previously reported (Boix-Besora et al., 2022; González-Domínguez et al., 2021; Steppert et al., 2016, 2017).

On the other hand, Figure 6 shows a molecular characterization of Gag VLPs obtained in each step. Final concentrated and purified Gag VLPs are clearly observed in cryo-TEM micrographs (Figure 6a), compared to other nanoparticles present in the sample. Gag VLPs are detected as spherical electrodense nanoparticles surrounded by a lipid membrane. On the other hand, as observed in the SDS-PAGE, as the process progresses, the sample corresponding to Gag-GFP is concentrated and other contaminating proteins are eliminated. Furthermore, in all steps the presence of Gag-eGFP was confirmed by Western blot (Figure 6b). The DLS also allowed to characterize the sample in each step of the process. It is observed how the peak narrows with respect to the production supernatant as the sample is increasingly purified (Figure 6c).
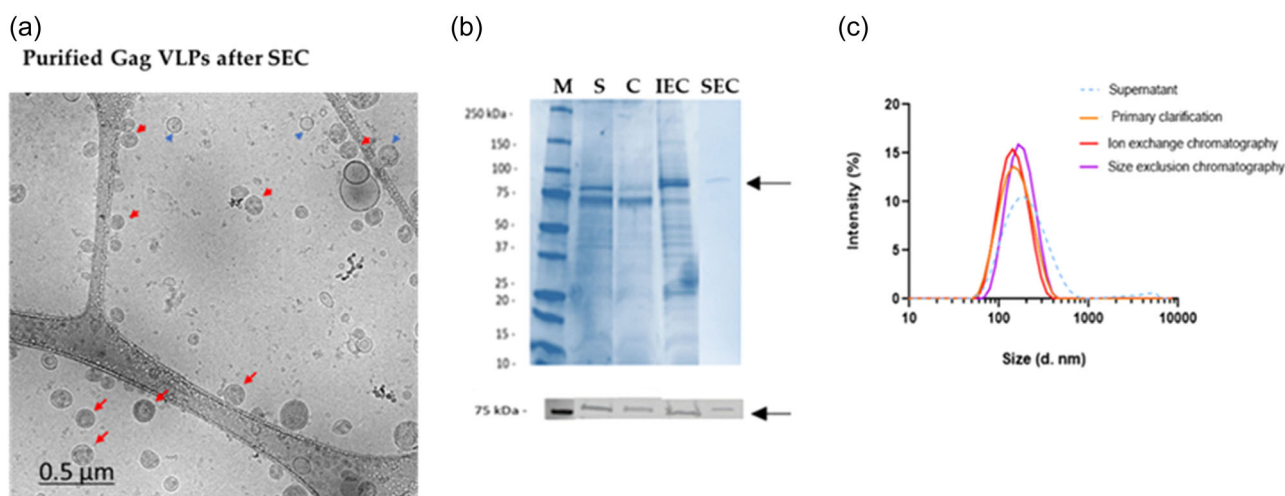
FIGURE 6 Molecular and biophysical characterization of Gag virus-like particles (VLPs) obtained in all steps of the final downstream processing (DSP) run (a) Cryo-TEM micrographs of purified material; (b) SDS-PAGE, p24 Western blot, (c) Dynamic light scattering (DLS) M, molecular weight standard; S, supernatant; C, clarified; IEC, elution peak 2 from Capto Q ImpRes and SEC, void volume from Sepharose 4FF. Red, blue, and black narrows indicate Gag VLPs, others nanoparticles and Gag-eGFP protein, respectively.

4 | CONCLUSIONS

The design of HIV-1 Gag-eGFP purification process, comparing different unit operations in each step has been achieved. In the primary clarification, it is possible to separate most of the cell aggregates and debris from the HIV-1 Gag-eGFP VLPs of the supernatant by means of depth filtration, without involving a significant loss of VLPs. This is refined by secondary clarification by filtration, and the dsDNA content is reduced. TFF enables further concentration, and more than 85% of dsDNA and total protein content removal. Capto Q ImpRes IEC shows the best results among all chromatography tested in capturing and purifying VLPs. Last, it is possible to achieve a higher purity, as well as a desalting and buffer exchange with the S4FF SEC. The process has shown a total recovery of 38% of Gag-eGFP VLPs with a total protein, and dsDNA removal of almost 100% from the crude supernatant. Along with a robust purification platform, efficient process monitoring tools are critical for process development and robust characterization to meet regulatory demands. Analytical methods such as DLS, NTA, flow virometry, electrophoresis, Western blot, and others performed in this study, have been widely applied to monitor multiple quality attributes of VLPs (González-Domínguez et al., 2021; Pereira Aguilar et al., 2020; Reiter et al., 2019). Overall, the DSP unit operations and the analytical tools studied here are suitable for large-scale manufacturing, supporting the use of the developed DSP bioprocess as platform for HIV-1 Gag VLPs purification.

DATA AVAILABILITY STATEMENT
The data that support the findings of this study are available from the corresponding author upon reasonable request.

ORCID
Elianet Lorenzo http://orcid.org/0000-0002-5442-0831

REFERENCES
Bandeira, V., Peixoto, C., Rodrigues, A. F., Cruz, P. E., Alves, P. M., Coroadinha, A. S., & Carrondo, M. J. T. (2012). Downstream processing of lentiviral vectors: Releasing bottlenecks. *Human Gene Therapy Methods*, 23(4), 255–263. https://doi.org/10.1089/hgtb.2012.059

Besnard, L., Fabre, V., Fettig, M., Gousseinov, E., Kawakami, Y., Laroudie, N., Scanlan, C., & Pattnaik, P. (2016). Clarification of vaccines: An overview of filter based technology trends and best practices. *Biotechnology Advances*, 34(1), 1–13. https://doi.org/10.1016/j.biotechadv.2015.11.005

Boix-Besora, A., Lorenzo, E., Lavado-García, J., Gòdia, F., & Cervera, L. (2022). Optimization, production, purification and characterization of HIV-1 GAG-based virus-like particles functionalized with SARS-CoV-2. *Vaccines*, 10(2), 250. https://doi.org/10.3390/vaccines10020250

Carvalho, S. B., Silva, R. J. S., Moleirinho, M. G., Cunha, B., Moreira, A. S., Xenopoulos, A., Alves, P. M., Carrondo, M. J. T., & Peixoto, C. (2019). Membrane-based approach for the downstream processing of influenza virus-like particles. *Biotechnology Journal*, 14, 8. https://doi.org/10.1002/biot.201800570

Carvalho, S. B., Silva, R. J. S., Moreira, A. S., Cunha, B., Clemente, J. J., Alves, P. M., Carrondo, M. J. T., Xenopoulos, A., & Peixoto, C. (2019). Efficient filtration strategies for the clarification of influenza virus-like particles derived from insect cells. *Separation and Purification Technology*, 218, 81–88. https://doi.org/10.1016/j.seppur.2019.02.040

Cervera, L., Fuenmayor, J., González-Domínguez, I., Gutiérrez-Granados, S., Segura, M. M., & Gòdia, F. (2015). Selection and optimization of transfection enhancer additives for increased virus-like particle production in HEK293 suspension cell cultures. *Applied Microbiology and Biotechnology*, 99(23), 9935–9949. https://doi.org/10.1007/s00253-015-6842-4

Cervera, L., Gonz Alez-Dom Inguez, I., Ia, M., Segura, M., & Godia, F. (2017). Intracellular characterization of Gag VLP production by transient transfection of HEK 293. *Biotechnol Bioeng*, 114(11), 2507–2517. https://doi.org/10.1002/bit.26367

Cervera, L., Gutiérrez-Granados, S., Martínez, M., Blanco, J., Gòdia, F., & Segura, M. M. (2013). Generation of HIV-1 Gag VLPs by transient transfection of HEK 293 suspension cell cultures using an optimized animal-derived component free medium. *Journal of Biotechnology*, 166(4), 152–165. https://doi.org/10.1016/j.jbiotec.2013.05.001

Fuenmayor, J., Gòdia, F., & Cervera, L. (2017). Production of virus-like particles for vaccines. *New Biotechnology*, 39, 174–180. https://doi.org/10.1016/j.nbt.2017.07.010

González-Domínguez, I., Lorenzo, E., Bernier, A., Cervera, L., Gòdia, F., & Kamen, A. (2021). A four-step purification process for gag vlps: from culture supernatant to high-purity lyophilized particles. *Vaccines*, 9(10), 1154. https://doi.org/10.3390/vaccines9101154

Jungbauer, A., & Hahn, R. (2004). Monoliths for fast bioseparation and bioconversion and their applications in biotechnology. *Journal of Separation Science*, 27(10–11), 767–778. https://doi.org/10.1002/jssc.200401812

Kramberger, P., Urbas, L., & Štrancar, A. (2015). Downstream processing and chromatography based analytical methods for production of vaccines, gene therapy vectors, and bacteriophages. *Human Vaccines & Immunotherapeutics*, 11(4), 1010–1021. https://doi.org/10.1080/21645515.2015.1009817

Lagoutte, P., Mignon, C., Donnat, S., Stadthagen, G., Mast, J., Sodoyer, R., Lugari, A., & Werle, B. (2016). Scalable chromatography-based purification of virus-like particle carrier for epitope based influenza A vaccine produced in *Escherichia coli*. *Journal of Virological Methods*, 232, 8–11. https://doi.org/10.1016/j.jviromet.2016.02.011

Lavado-García, J., Jorge, I., Cervera, L., Vázquez, J., & Gòdia, F. (2020). Multiplexed quantitative proteomic analysis of HEK293 provides insights into molecular changes associated with the cell density effect, transient transfection, and virus-like particle production. *Journal of Proteome Research*, 19(3), 1085–1099. https://doi.org/10.1021/acs.jproteome.9b00601

Lima, T. M., Souza, M. O., & Castilho, L. R. (2019). Purification of flavivirus VLPs by a two-step chomatographic process. *Vaccine*, 37(47), 7061–7069. https://doi.org/10.1016/j.vaccine.2019.05.066

Lin, S. Y., Chiu, H. Y., Chiang, B. L., & Hu, Y. C. (2015). Development of EV71 virus-like particle purification processes. *Vaccine*, *33*(44), 5966–5973. https://doi.org/10.1016/j.vaccine.2015.04.077

Mittal, M., Banerjee, M., Lua, L. H., & Rathore, A. S. (2022). Current status and future challenges in transitioning to continuous bioprocessing of virus-like particles. *Journal of Chemical Technology & Biotechnology*, *97*(9), 2376–2385. https://doi.org/10.1002/jctb.6821

Moleirinho, M. G., Rosa, S., Carrondo, M. J. T., Silva, R. J. S., Hagner-McWhirter, Å., Ahlén, G., Lundgren, M., Alves, P. M., & Peixoto, C. (2018). Clinical-Grade oncolytic adenovirus purification using polysorbate 20 as an alternative for cell lysis. *Current Gene Therapy*, *18*(6), 366–374. https://doi.org/10.2174/156652321866181109141257

Moleirinho, M. G., Silva, R. J. S., Alves, P. M., Carrondo, M. J. T., & Peixoto, C. (2019). Current challenges in biotherapeutic particles manufacturing. *Expert Opinion on Biological Therapy*, *20*(5), 451–465. https://doi.org/10.1080/14712598.2020.1693541

Nooraei, S., Bahrulolum, H., Hoseini, Z. S., Katalani, C., Hajizade, A., Easton, A. J., & Ahmadian, G. (2021). Virus-like particles: Preparation, immunogenicity and their roles as nanovaccines and drug nanocarriers. *Journal of Nanobiotechnology*, *19*(1), 59. https://doi.org/10.1186/s12951-021-00806-7

Nweke, M. C., McCartney, R. G., & Bracewell, D. G. (2017). Mechanical characterisation of agarose-based chromatography resins for bio-pharmaceutical manufacture. *Journal of Chromatography A*, *1530*, 129–137. https://doi.org/10.1016/j.chroma.2017.11.038

Peixoto, C., Sousa, M. F. Q., Silva, A. C., Carrondo, M. J. T., & Alves, P. M. (2007). Downstream processing of triple layered rotavirus like particles. *Journal of Biotechnology*, *127*(3), 452–461. https://doi.org/10.1016/j.jbiotec.2006.08.002

Pereira Aguilar, P., Reiter, K., Wetter, V., Steppert, P., Maresch, D., Ling, W. L., Satzer, P., & Jungbauer, A. (2020). Capture and purification of human immunodeficiency virus-1 virus-like particles: Convective media vs porous beads. *Journal of Chromatography A*, *1627*, 461378. https://doi.org/10.1016/j.chroma.2020.461378

Pereira Aguilar, P., Schneider, T. A., Wetter, V., Maresch, D., Ling, W. L., Tover, A., Steppert, P., & Jungbauer, A. (2019). Polymer-grafted chromatography media for the purification of enveloped virus-like particles, exemplified with HIV-1 gag VLP. *Vaccine*, *37*(47), 7070–7080. https://doi.org/10.1016/j.vaccine.2019.07.001

Reiter, K., Aguilar, P. P., Wetter, V., Steppert, P., Tover, A., & Jungbauer, A. (2019). Separation of virus-like particles and extracellular vesicles by flow-through and heparin affinity chromatography. *Journal of Chromatography A*, *1588*, 77–84. https://doi.org/10.1016/j.chroma.2018.12.035

Reiter, K., Pereira Aguilar, P., Grammelhofer, D., Joseph, J., Steppert, P., & Jungbauer, A. (2020). Separation of influenza virus-like particles from baculovirus by polymer-grafted anion exchanger. *Journal of Separation Science*, *43*(12), 2270–2278. https://doi.org/10.1002/jssc.201901215

Schwartz, S., Campbell, M., Nasioulas, G., Harrison, J., Felber, B. K., & Pavlakis, G. N. (1992). Mutational inactivation of an inhibitory sequence in human immunodeficiency virus type 1 results in Rev-independent gag expression. *Journal of Virology*, *66*(12), 7176–7182. https://doi.org/10.1128/jvi.66.12.7176-7182.1992

Segura, M. M., Mangion, M., Gaillet, B., & Garnier, A. (2013). New developments in lentiviral vector design, production and purification. *Expert Opinion on Biological Therapy*, *13*(7), 987–1011. https://doi.org/10.1517/14712598.2013.779249

Steppert, P., Burgstaller, D., Klausberger, M., Berger, E., Aguilar, P. P., Schneider, T. A., Kramberger, P., Tover, A., Nöbauer, K., Razzazi-Fazeli, E., & Jungbauer, A. (2016). Purification of HIV-1 gag virus-like particles and separation of other extracellular particles. *Journal of Chromatography A*, *1455*, 93–101. https://doi.org/10.1016/j.chroma.2016.05.053

Steppert, P., Burgstaller, D., Klausberger, M., Kramberger, P., Tover, A., Berger, E., Nöbauer, K., Razzazi-Fazeli, E., & Jungbauer, A. (2017). Separation of HIV-1 gag virus-like particles from vesicular particles impurities by hydroxyl-functionalized monoliths. *Journal of Separation Science*, *40*(4), 979–990. https://doi.org/10.1002/jssc.201600765

Venereo-Sanchez, A., Gilbert, R., Simoneau, M., Caron, A., Chahal, P., Chen, W., Ansorge, S., Li, X., Henry, O., & Kamen, A. (2016). Hemagglutinin and neuraminidase containing virus-like particles produced in HEK-293 suspension culture: An effective influenza vaccine candidate. *Vaccine*, *34*(29), 3371–3380. https://doi.org/10.1016/j.vaccine.2016.04.089

Vicente, T., Roldão, A., Peixoto, C., Carrondo, M. J. T., & Alves, P. M. (2011). Large-scale production and purification of VLP-based vaccines. *Journal of Invertebrate Pathology*, *107*, S42–S48. https://doi.org/10.1016/j.jip.2011.05.004

Zaveckas, M., Goda, K., Ziogiene, D., & Gedvilaite, A. (2018). Purification of recombinant trichodysplasia spinulosa–associated polyomavirus VP1-derived virus-like particles using chromatographic techniques. *Journal of Chromatography B*, *1090*, 7–13. https://doi.org/10.1016/j.jchromb.2018.05.007

Zhao, M., Vandersluis, M., Stout, J., Haupts, U., Sanders, M., & Jacquemart, R. (2019). Affinity chromatography for vaccines manufacturing: Finally ready for prime time? *Vaccine*, *37*(36), 5491–5503. https://doi.org/10.1016/j.vaccine.2018.02.090

SUPPORTING INFORMATION

Additional supporting information can be found online in the Supporting Information section at the end of this article.